

Dependence of transport on adatom location for armchair-edge graphene nanoribbons

Xiongwen Chen,^{1,2} Kehui Song,² Benhu Zhou,¹ Haiyan Wang¹ and Guanghui Zhou^{1,3*}

¹*Department of Physics and Key Laboratory for Low-Dimensional Quantum Structures and Manipulation (Ministry of Education), Hunan Normal University, Changsha 410081, China*

²*Department of Physics and Electronic Information Science, Huaihua University, Huaihua 418008, China and*

³*International Center for Materials Physics, Chinese Academy of Sciences, Shenyang 110015, China*

Abstract

We study the transport property for armchair-edge graphene nanoribbons (AGNRs) with an adatom coupling to a semi-infinite quantum wire. Using the nonequilibrium Green's function approach with tight-binding approximation, we demonstrate that the tunneling current through the system is sensitively dependent on both the AGNR width and adatom location. Interestingly, when the adatom locates onto a carbon atom in the 3rd chain from the edge of a metallic AGNR, the system shows a transmission gap accompanied by a threshold voltage in $I - V$ curve like a semiconducting AGNR. This effect may be useful in scanning tunneling microscopy experimental characterization on graphene samples.

*Electronic address: ghzhou@hunnu.edu.cn

Recently, the successful fabrication of graphene in experiment¹ results in intensive attention due to its unique properties² and potential applications in electromechanical resonator,³ p - n junction,⁴ transistor⁵ and thermoelectric power devices,⁶ etc. However, due to the absence of gap in the energy spectrum, graphene is difficult to be used in the electronic device which requires precise control of carrier type and transport behavior. Fortunately, GNRs, finite width of graphene, open a gap in the energy spectrum because of the quantum confinement effect,^{2,7} remedying the drawback of graphene. Thus, GNRs are more suitable promising materials for the design of electronic devices.⁸⁻¹² According to the atomic configuration of the edge, GNRs are classified into two types of AGNR and zigzag-edge GNR (ZGNR). It has been shown that a pristine AGNR exhibits either metallic or semiconducting nature with a gap depending on the number of elementary cells N from one edge to another,^{13,14} i.e., an AGNR is metallic if $N=3p-1$ (p is an integer) otherwise ($N=3p-2$ or $3p-3$) semiconducting, while ZGNRs always maintain metallic behavior with localized states near the Fermi level.¹³

In this Letter, we study the transport property for AGNRs with an impurity atom absorbed on the top of a carbon atom in AGNR. As shown in Fig. 1(a), like the model proposed for STM experiment on graphene¹⁵⁻¹⁸ or surface of materials,¹⁹ a semi-infinite quantum wire (as a probe) couples to an AGNR via an adatom. In Fig. 1(b), the (red) dashed line rectangle is the periodical unit which is composed of N elementary cells for AGNR,^{13,14} where cell (m, n) contains four carbon atoms labeled as β, γ, λ and δ connected by the (blue) thick solid line. Using the NEGF approach with the help of tight-binding approximation, we demonstrate that the tunneling current through the system is sensitively dependent on both the width of AGNR and the location of the adatom on it. Interestingly, when the adatom locates onto a carbon atom in the $3j$ th chain from the edge of a metallic AGNR, system shows a transmission gap accompanied by a threshold voltage in the current-voltage curve, which is a conspicuous semiconducting transport behavior in the semiconducting-AGNR-based system. This effect may be useful in the STM experimental characterization on the GNR samples and in the application of graphene-based nanodevices.

The Hamiltonian for this AGNR-based system reads

$$H = H_W + H_G + H_I + H_T, \quad (1)$$

where $H_W = \sum_{j=1}^{\infty} \mu_1 a_j^\dagger a_j - \sum_{j=1}^{\infty} t_1 (a_j^\dagger a_{j+1} + h.c.)$ for the semi-infinite wire with chemical potential μ_1 and hopping energy t_1 ; $H_G = \sum_{m,n,\alpha} \mu_2 c_{m,n,\alpha}^\dagger c_{m,n,\alpha} - \sum_{\langle \cdot, \cdot \rangle} t_2 (c_{m,n,\alpha}^\dagger c_{m',n',\alpha'} + h.c.)$ for the π -band electron of AGNR with chemical potential μ_2 , where $\langle \cdot, \cdot \rangle$ denotes summing over nearest-neighbor sites

with hopping integral t_2 ; $H_I = \epsilon_0 d^\dagger d$ for the adatom with single energy level ϵ_0 couples to both site $j=1$ of the wire and lattice site α in AGNR respectively through coupling strength ν_1 and ν_2 with tunneling Hamiltonian $H_T = (\nu_1 d^\dagger a_1 + \nu_2 d^\dagger c_{m,n,\alpha} + h.c.)$. The potential difference between the wire and AGNR (via substrate) is related to the applied bias voltage as $U = \mu_1 - \mu_2$.

Therefore, for the AGNR-based system of an adatom located in cell n , the tunneling current can be expressed as

$$I_n(U) = \frac{2e}{h} \int_{\mu_2}^{\mu_1} d\omega [f_1(\omega - \mu_1) - f_2(\omega - \mu_2)] T_n(\omega), \quad (2)$$

where $f_{1(2)}$ is the Fermi-Dirac distribution function for the wire (AGNR), T_n is the n -dependent transmission probability which can be obtained by solving full Hamiltonian (1) by means of NEGF within the nearest-neighbor tight-binding scheme.

The isolated retarded Green's function (GF) matrix for the system is defined as

$$g^r(\omega) = \begin{bmatrix} g_{11}^r(\omega) & 0 & 0 \\ 0 & g_{00}^r(\omega) & 0 \\ 0 & 0 & g_{m,n,\alpha}^r(\omega) \end{bmatrix}, \quad (3)$$

where $g_{00}^r(\omega) = (\omega - \epsilon_0 + i0^\dagger)^{-1}$ is the GF for the adatom, $g_{11}^r(\omega)$ and $g_{m,n,\alpha}^r(\omega)$ are GF for the edge site ($j=1$) of the wire and site α in cell n , respectively. Using the NEGF, one finds^{16,17}

$$g_{11}^r(\omega) = \frac{\omega - \mu_1}{2t_1^2} - i \frac{\sqrt{4t_1^2 - (\omega - \mu_1)^2}}{2t_1^2} \quad (4)$$

with local density of states (LDOS) $\rho_{11}(\omega) = -\frac{1}{\pi} \text{Im}[g_{11}^r(\omega)]$ at site $j=1$ in the wire and

$$g_{m,n,\alpha}^r(\omega) = \sum_{k_x, k_q, \pm} \frac{\psi_{m,n,\alpha}(k_x, k_q) \psi_{m,n,\alpha}^*(k_x, k_q)}{\omega - E^\pm + i0^\dagger} \quad (5)$$

with LDOS $\rho_{m,n,\alpha}(\omega) = -\frac{1}{\pi} \text{Im}[g_{m,n,\alpha}^r(\omega)]$ at site α in the n th cell of AGNR.

Further, based on the nearest-neighbor tight-binding approximation, one can obtain^{13,14} the π -electron energy spectrum in the low-energy limit as

$$E^\pm = \mu_2 \pm t_2 \sqrt{1 - 4\cos\frac{k_q}{2}\cos\frac{3k_x}{2} + 4\cos^2\frac{k_q}{2}}, \quad (6)$$

and the wavefunction

$$\psi_{m,n,\alpha}(k_x, k_q) = C \begin{cases} e^{i\varphi_\alpha(k_x, k_q)} \sin(k_q n), & \alpha = \beta, \gamma \\ e^{i\varphi_\alpha(k_x, k_q)} \sin[k_q(n - 1/2)], & \alpha = \lambda, \delta \end{cases} \quad (7)$$

under the hard-wall boundary condition with normalized constant $C=[2(N+1)]^{-1/2}$, where φ_α is an arbitrary function and the carbon-carbon bond length has been set to unitary. The wavevector k_x is continuous and the y-direction wavevector is discretized as $k_q=q\pi/(N+1)$ with subband index number $q=1, 2, \dots, N$ for a perfect AGNR. Hence, the energy gap ΔE between the q th conduction and valence band is given by $2t_2|1 - 2\cos(k_q/2)|$.

Moreover, the retarded self-energy matrix has four nonzero elements of $\Sigma_{1,0(0,1)}^r=\nu_1$ ($\Sigma_{0,\alpha(\alpha,0)}^r=\nu_2$), which describes the tunneling between the adatom and wire (AGNR), respectively. Therefore, by employing Dyson equation $G^r=[(g^r)^{-1}-\Sigma^r]^{-1}$, one gets the full retarded GF for the adatom $G_{00}^r(\omega)$ and lastly obtains the electronic transmission probability $T_n=4\Gamma_{01}(\omega)|G_{00}^r(\omega)|^2\Gamma_{02}(\omega)$ with linewidth functions $\Gamma_{01}(\omega)=\pi|\nu_1|^2\rho_{11}(\omega)$ and $\Gamma_{02}(\omega)=\pi|\nu_2|^2\rho_{m,n,\alpha}(\omega)$.

In the following we present some numerical examples for the systems with $N=7$ and 8 AGNR, respectively. The potentials $\mu_1=-\mu_2=U/2$ and the hopping energies $t_1=t_2=t$, where we have set the origin of energy as the Fermi energy ($E_F=0$) at equilibrium case. In our model, when the adatom energy ϵ_0 deviates from E_F along the positive or negative direction, the impurity scattering for electronic transmission suppresses the amplitude of tunneling current. But this do not change the major characteristics for electronic transmission which is determined mainly by the energy spectrum of AGNRs. Thus, to obtain the essence of transport property for our system, we fix ϵ_0 at E_F and set the coupling strength $\nu_1=\nu_2=0.5$ without loss generality.

In Fig. 2, transmission probability T_n versus energy ω (in units of t) at equilibrium case of $\mu_{1(2)}=0$ and tunneling current I_n (in units of e/h) versus bias voltage U for different adatom positions are depicted, respectively. Obviously, the transport property of the system strongly depend on the width (or number of cells N) of AGNR and the adatom location (n) on it. As shown in Fig. 2(a) for the system with $N=7$, the semiconducting nature is always kept regardless of n , which is signed by a transmission gap $\Delta\omega \approx 0.22$ around $E_F=0$ and a series of signature peaks from subbands. This gap can be determined from the minimal energy gap ΔE_{min} . Consequently, as shown in Fig. 2(b), only when the applied bias voltage U is above $\Delta\omega/2$, carriers in the highest valence band ($q=5$) can jump to Fermi level and take part in transport, thus there exists a threshold voltage $U_c \approx 0.11$ for the semiconducting system. As U increases, other subbands become propagating accordingly one by one, which results in broken-line signs in $I-U$ curve in contrast to the smooth $I-U$ characteristic in the previously studied similar graphene-based system.^{16,17}

In contrast, for $N=8$ the system shows a metallic behavior with a zero transmission gap [see

Fig. 2(c)] and linear I - U characteristics [Fig. 2(d)] when the adatom is located at site β or γ in cells of $n=1,2,4$ because that the sixth ($q=6$) valence band and conduction band meet at the Fermi energy with a zero gap.¹¹ Interestingly, when the adatom is located at cell $n=3$, there exists a wide transmission gap of $\Delta\omega\approx 0.54$ associated with a large threshold voltage $U_c\approx 0.27$ for the system [see (black) solid lines in Fig. 2(c) and 2(d)]. In this case, the metallic-AGNR-based system surprisingly exhibits semiconducting behavior. Actually, this phenomenon can be explained by wavefunction (7). As shown by the (black) solid line in Fig. 3(a), for metallic AGNR with $N=8$, the adatom locating at site β or γ in cell $n=3$ results in $|\psi_{m,3,\beta(\gamma)}(k_x, k_y)|^2=0$, hence the sixth (gapless) subband does not contribute to transport in this case. Generally, for any metallic-AGNR-based system, the semiconducting transport behavior exists only if the adatom is located at the positions of carbons in cells of $n = 3j$ for $\alpha = \beta(\gamma)$ and $3j - 1$ for $\alpha = \lambda(\delta)$ with integer j , respectively. In other words, the zero gap subband is not effective when the adatom is located at the $3j$ th chain from the edge of AGNR because $|\psi_{m,n,\alpha}|^2=0$ as $q = 2(N + 1)/3$. Comparatively, $|\psi_{m,n,\alpha}|^2$ at the q' th subband with $q'=[2(N - 1)/3]$ (where $[\cdot]$ rounds a number to the nearest integer) begins to have nonzero value from the Fermi level. Therefore, the threshold voltage U_c is taken as $t_2|1 - 2\cos[q'\pi/(2N+2)]|$ depending on the metallic AGNR width N . Of course, this transition from metallic to semiconducting does not exist for either metallic AGNRs transport in the graphene-plane⁹⁻¹² or graphene-based systems.¹⁵⁻¹⁸

On the other hand, as an application of this transition effect found here, firstly one can find the location of an adatom on an AGNR sample in a STM experiment. Further, for a set of AGNRs with same p , the metallic AGNR possesses the widest ΔE_{min} when its zero gap subband is not absent as shown by the (black) solid line in Fig. 3(b). Therefore, when ΔE_{min} is small enough to be neglected, all AGNRs can be treated as graphene. The turning point is around $N=400$ which corresponds the width of AGNR about 100 nm. Moreover, because of quantum confinement, the difference between energy levels in the wider AGNRs is smaller than that of narrower AGNRs. So in the wider AGNRs, the number of conduction channels within bias voltage window changes less abruptly, which gives rise to a smooth I - U curve as shown with the (black) solid lines in Fig. 4(b) and 4(d) despite the existence of weak oscillating in transmission spectrum displayed in Fig. 4(a) and 4(c). Therefore, the smooth I - U curve is a visible symbol for the wider AGNRs compared to the broken-line signs in I - U curve for the narrower AGNRs [see (blue) dot and (red) dashed lines in Fig. 4(b) and 4(d)]. However, a threshold voltage U_c (decreases as N increases) always exists when $n=3j$ for $\alpha=\beta(\gamma)$ and $3j - 1$ for $\alpha=\lambda(\delta)$, respectively, even though N is large enough

to neglect the finite-size effect [see Fig. 4(d)] in our model. Therefore, one can use the magnitude of U_c to identify an AGNR sample in practical STM experiment by our setup shown in Fig.1.

In conclusion, we have considered an AGNR-based system with a single adatom couples to both a semi-infinite wire and an AGNR. Using the NEGF technique within the nearest-neighbor tight-binding scheme, it is found that the tunneling current of the system is sensitively dependent on both the width of AGNR and the location of adatom on it. Interestingly, when the adatom is on a carbon atom in the $3j$ th chain from the edge of a metallic AGNR, a metallic-AGNR-based system always exists a transmission gap and consequently followed by a threshold voltage U_c in I - U curve, which is a conspicuous semiconducting transport behavior in the semiconducting-AGNR-based system. Although the values of transmission gap and U_c in real situation may slightly differ from our theoretical prediction due to the unsaturated edge bonds or other factors which induce the variation of subbands for GNRs,⁸⁻¹² we believe that the main point here is qualitatively sound. And this effect may be useful in the STM experimental characterization on AGNRs and in the application of graphene-based nanodevices.

We thank Dr. Dongsheng Tang for insightful discussions. This work was supported by the National Natural Science Foundation of China (Grant No. 10974052), the Scientific Research Fund of Hunan Provincial Education Department (Grant No. 09B079), and the Program for Changjiang Scholars and Innovative Research Team in University (PCSIRT, No. IRT0964).

-
- [1] K. S. Novoselov, A. K. Geim, S. V. Morozov, D. Jiang, Y. Zhang, S. V. Dubonos, I. V. Grigorieva, and A. A. Firsov, *Science* **306**, 666 (2004); K. S. Novoselov, A. K. Geim, S. V. Morozov, D. Jiang, M. I. Katsnelson, I. V. Grigorieva, S. V. Dubonos, and A. A. Firsov, *Nature (London)* **438**, 197 (2005).
- [2] A. H. Castro Neto, F. Guinea, N. M. R. Peres, K. S. Novoselov, and A. K. Geim, *Rev. Mod. Phys.* **81**, 109 (2009).
- [3] J. S. Bunch, A. M. van der Zande, S. S. Verbridge, I. W. Frank, D. M. Tanenbaum, J. M. Parpia, H. G. Craighead, P. L. McEuen, *Science* **315**, 490 (2007).
- [4] J. R. Williams, L. DiCarlo, and C. M. Marcus, *Science* **317**, 638 (2007).
- [5] Q. Yan, B. Huang, J. Yu, F. Zheng, J. Zang, J. Wu, B.-L. Gu, F. Liu, and W. H. Duan, *Nano Lett.* **7**, 1469 (2007).
- [6] D. Dragoman and M. Dragoman, *Appl. Phys. Lett.* **91**, 203116 (2007).
- [7] Y.-W. Son, M. L. Cohen, and S. G. Louie, *Phys. Rev. Lett.* **97**, 216803 (2006).
- [8] Z. P. Xu, Q. S. Zheng, and G. H. Chen, *Appl. Phys. Lett.* **90**, 223115 (2007).
- [9] D. Basu, M. J. Gilbert, L. F. Register, S. K. Banerjee, and A. H. MacDonald, *Appl. Phys. Lett.* **92**, 042114 (2008).
- [10] Z. Z. Zhang, K. Chang, and K. S. Chan, *Appl. Phys. Lett.* **93**, 062106 (2008).
- [11] P. Zhao, J. Chauhan, and J. Guo, *Nano Lett.* **9**, 684 (2009).
- [12] M. Yamamoto, and K. Wakabayashi, *Appl. Phys. Lett.* **95**, 082109 (2009).
- [13] L. Malysheva and A. Onipko, *Phys. Rev. Lett.* **100**, 186806 (2008); A. Onipko, *Phys. Rev. B* **78**, 245412 (2008).
- [14] Y. O. Klymenko and O. Shevtsov, *Eur. Phys. J. B* **69**, 383 (2009).
- [15] Z. F. Wang, R. Xiang, Q. W. Shi, J. Yang, X. Wang, J. G. Hou, and J. Chen, *Phys. Rev. B* **74**, 125417 (2006).
- [16] T. Fukuda, H. Oymak, and J. Hong, *J. Phys.: Condens. Matter* **20**, 055207 (2008).
- [17] N. M. R. Peres, S.-W. Tsai, J. E. Santos, and R. M. Ribeiro, *Phys. Rev. B* **79**, 155442 (2009); N. M. R. Peres, L. Yang, and S.-W. Tsai, *New J. Phys.* **11**, 095007 (2009).
- [18] K. Saha, I. Paul, and K. Sengupta, *Phys. Rev. B* **81**, 165446 (2010).
- [19] T. Fukuda, H. Oymak, and J. Hong, *Phys. Rev. B* **75**, 195428 (2007).

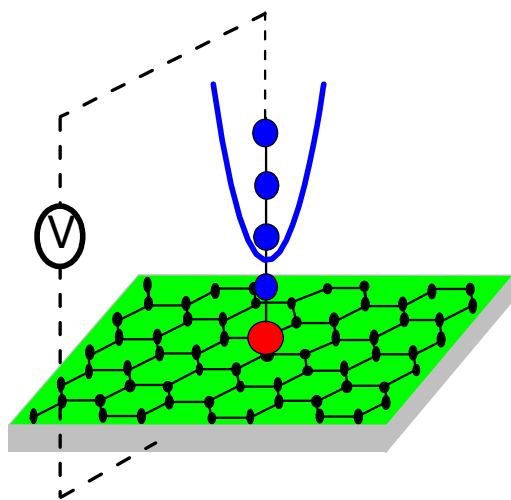
List of Figure Captions:

Fig.1: (Color online) (a) Electrons tunneling from a semi-infinite wire to an AGNR on substrate via an (red) adatom on a carbon site of AGNR. (b) The (red) dashed line rectangle represents the m th unit along the x -direction, in which the elementary cell n along the y -direction is composed of four carbon atoms ($\beta, \gamma, \lambda, \delta$) connected by blue line.

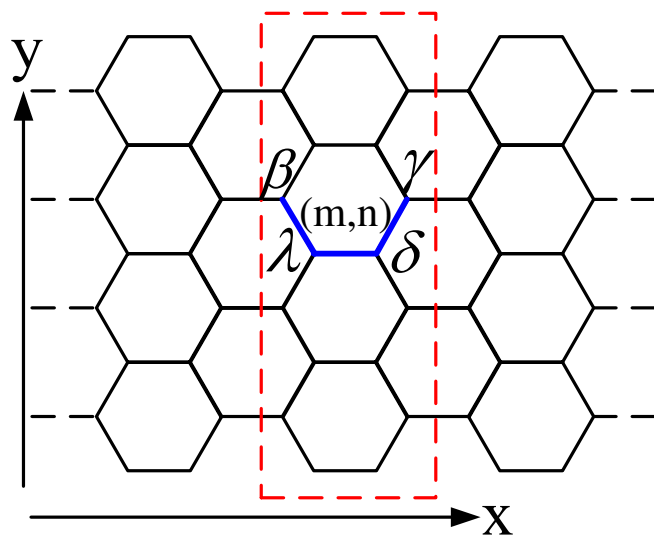
Fig.2: (Color online) Transport property of the system with different AGNR width N and the adatom position $n(\beta, \gamma)$. Left for transmission probability $T_n(\omega)$ and right for tunneling current $I_n(U)$, where (a) and (b) for $N=7$, (c) and (d) for $N=8$.

Fig.3: (Color online) (a) Squared wavefunctions for different subband indices in metallic AGNR of $N=8$ as a function of adatom position. (b) Minimal energy gap as a function of AGNR width. Note that the zero energy gap in pristine metallic AGNR ($N=3p - 1$) is absent in the corresponding adatom-attached ribbon as indicated by (black) solid line.

Fig.4: (Color online) Transport property for metallic-AGNR-based system with different N and n , where (a) and (b) for $n=1$, (c) and (d) for $n=3$.



(a)



(b)

